

## Comparative Structural Connectivity Spectra Analysis (CoSCoSA) Models of Steroid Binding to the Corticosteroid Binding Globulin

Richard D. Beger,\* Dan A. Buzatu, Jon G. Wilkes, and Jackson O. Lay, Jr.

Division of Chemistry, National Center for Toxicological Research, Food and Drug Administration,  
Jefferson, Arkansas 72079-9502

Received March 11, 2002

A three-dimensional quantitative spectrometric data-activity relationship (3D-QSDAR) model was developed that is built by combining NMR spectral information with structural information in a 3D-connectivity matrix. The 3D-connectivity matrix is built by displaying all possible carbon-to-carbon connections with their assigned carbon NMR chemical shifts and distances between the carbons. Selected 2D  $^{13}\text{C}$ - $^{13}\text{C}$  Correlation Spectroscopy (COSY) (through-bond nearest neighbors) and selected theoretical 2D  $^{13}\text{C}$ - $^{13}\text{C}$  distance connectivity spectral slices from the 3D-connectivity matrix to produce a relationship among the spectral patterns for 30 steroids binding to corticosteroid binding globulin. We call this technique a comparative structural connectivity spectra analysis (CoSCoSA) modeling. A CoSCoSA principal component linear regression model based on the combination of  $^{13}\text{C}$ - $^{13}\text{C}$  COSY and  $^{13}\text{C}$ - $^{13}\text{C}$  distance spectra principal components (PCs) had an  $r^2$  of 0.96 and a leave-one-out (LOO) cross-validation  $q^2$  of 0.92. A CoSCoSA parallel distributed artificial neural network (PD-ANN) model based on the combination of  $^{13}\text{C}$ - $^{13}\text{C}$  COSY and  $^{13}\text{C}$ - $^{13}\text{C}$  distance spectra had an  $r^2$  of 0.96, a leave-three-out  $q_3^2$  of 0.78, and a leave-ten-out  $q_{10}^2$  of 0.73. CoSCoSA modeling attempts to uniquely combine the quantum mechanics information from the NMR chemical shifts with internal molecular atom-to-atom distances into an accurate modeling technique. The CoSCoSA modeling technique has the flexibility and accuracy to outperform the cross-validated variance  $q^2$  of previously published quantitative structure–activity relationship (QSAR), quantitative spectral data-activity relationship (QSDAR), self-organizing map (SOM), and electrotopological state (E-state) models.

### INTRODUCTION

Many different types of models have been developed to predict the binding activity for the compound-receptor system of the corticosterone binding globulin.<sup>1</sup> These corticosteroid binding globulin models include the standard quantitative structure–activity relationship (QSAR),<sup>2</sup> the hybrid electrotopological state (E-state),<sup>3</sup> the self-organizing map (SOM),<sup>4</sup> and the combination QSAR E-state models.<sup>5</sup> Previously, we have demonstrated that  $^{13}\text{C}$  NMR spectrometric data can be used to produce reliable quantitative spectrometric data-activity relationship (QSDAR) models of binding to the corticosterone binding globulin,<sup>6</sup> aromatase enzyme,<sup>7</sup> and aryl hydrocarbon receptor.<sup>8</sup> These comparative spectral analysis (CoSA) models using simulated  $^{13}\text{C}$  NMR data yielded higher cross-validated correlations than were seen with comparative molecular field analysis (CoMFA) methods and comparative structure assigned spectra analysis (CoSASA).<sup>6,7</sup>

Our previous QSDAR CoSA model for the 30 corticosterone binding globulin steroids was significantly robust with an  $r^2$  of 0.80 and a  $q^2$  of 0.78,<sup>6</sup> but we believed we could do better if we were able to add structural information to the one-dimensional CoSA models. We added structurally assigned chemical shift to the backbone of steroids, and we obtained a CoSASA model with an  $r^2$  of 0.80 and a LOO cross-validation  $q^2$  of 0.73.<sup>6</sup> We thought the addition of two-dimensional structural information would drastically improve

the model, but the results were approximately the same for the 1D CoSA and 2D CoSASA models. In this paper, we demonstrate CoSCoSA modeling is an improvement over previous CoSA, CoSASA, and CoMFA models of binding to the corticosterone binding globulin.

The power of QSDAR is that it is unnecessary to solve any quantum mechanical calculations or use the structures of molecules for electrostatic calculations as is done in QSAR techniques.<sup>2,9–13</sup> QSAR is based on the assumption that there is a relationship between structure and activity of a compound. QSAR modeling results show that receptor binding of a compound can be predicted from a combination of electrostatics potentials and geometrical structural analysis.<sup>2,12,13</sup>

$^{13}\text{C}$  nuclear magnetic resonance (NMR) chemical shifts have been used to predict and refine chemical structures.<sup>14,15</sup> Conversely, the chemical structure of a compound has been used to predict its  $^{13}\text{C}$  NMR chemical shifts.<sup>16</sup> The  $^{13}\text{C}$  NMR spectrum of a compound contains frequencies that correspond directly to the quantum mechanical properties of every  $^{13}\text{C}$  nuclear magnetic moment in a chemical structure. The quantum mechanical description of a molecule depends largely on its electrostatic features and three-dimensional geometry.<sup>17</sup>

Current QSAR and structure–activity relationship (SAR) models use computer modeling of the molecule or break the molecule into secondary structural pieces.<sup>8–12,18–20</sup> Many calculations are used in QSAR, SOM, or E-states models. Using a specific molecular structure for computer modeling

\* Corresponding author phone: (870)543-7080; fax: (870)543-7686; e-mail: rbeger@nctr.fda.gov.

of each compound dramatically extends the number of calculations required to define the model. Moreover, the selection of the most appropriate 3D structure for each molecule requires a number of assumptions. The necessary simplifying assumptions in some cases give results that are hard to replicate or are inaccurate.

The present research initiative avoids some of the foregoing problems by providing a method for predicting a biological activity of a molecule, by using the  $^{13}\text{C}$  NMR spectral data for a test compound and adding the molecules structural connectivity information into a 3D-connectivity matrix. The 3D-connectivity matrix is built by displaying all possible carbon-to-carbon connections and their assigned carbon NMR chemical shifts, so that the  $x$ -axis is the chemical shifts of carbon  $i$ , the  $y$ -axis is the chemical shifts of carbon  $j$ , and the  $z$ -axis is the distance between carbon  $i$  and carbon  $j$  ( $r_{ij}$ ). Each carbon-to-carbon connection in the 3D matrix acts as a constraint on the structure of the molecule. The number of carbon-to-carbon constraints in a 3D-connectivity matrix increases as the square of the number of carbon atoms in the molecule. There are  $3N-6$  degrees of freedom in a molecule. When the number of structural constraints exceeds the number of degrees of freedom, the information in a 3D-connectivity matrix is said to over determine the structure of a molecule. For molecules the size of steroids, it is possible to reduce the detail in the 3D-connectivity matrix without losing access to the implicit structure-activity characteristics available from this way of describing them. One way to reduce the information is to reduce the 3D matrix into a set of 2D planes. We decided to reduce the 3D-matrix into four 2D spectral planes. The first 2D plane was the nearest neighbor through-bond connectivity plane. The three other 2D planes were constructed from compressing distance information on the  $z$ -axis, one for all short atom-to-atom connections ( $2.0 \text{ \AA} < r_{ij} < 3.6 \text{ \AA}$ ), one for all medium atom-to-atom connections ( $3.6 \text{ \AA} < r_{ij} < 6.9 \text{ \AA}$ ), and one for all long atom-to-atom connections ( $r_{ij} > 6.9 \text{ \AA}$ ). Similarities between the pattern of 2D spectral data associated with the biological activity of the training set compounds and the spectral data for the test compound are detected by principal component regression to determine whether the compound is predicted to exhibit the biological activity.

Standard NMR instrumental techniques include 2D  $^1\text{H}$ - $^1\text{H}$  COSY<sup>21</sup> experiments in which connectivity relationships through three bonds are found for nearest neighbor protons with an off diagonal cross-peak. This experiment is similar to 2D  $^{13}\text{C}$ - $^{13}\text{C}$  COSY experiments that contain analogous through bond connectivity spectral patterns. For the 3D-QSDAR methods developed in this work, the information contents of such COSY experiments are paralleled in the shortest distance layer of the connectivity matrix. Using the structurally assigned predicted spectra and adding the nearest neighbor information as cross-peaks produces this layer.

Our 3D-QSDAR predictive method also bears comparison to several other multidimensional NMR experimental techniques.  $^{13}\text{C}$ - $^{13}\text{C}$  COSY experiments have similarities to 2D  $^1\text{H}$ - $^{13}\text{C}$  heteronuclear single quantum correlation (HSQC)<sup>22</sup> and  $^1\text{H}$ - $^{13}\text{C}$  heteronuclear multiple quantum correlation (HMQC)<sup>23</sup> NMR experiments that show the connectivity for carbons and their attached protons. In practice, 2D  $^{13}\text{C}$ - $^{13}\text{C}$  COSY are seldom run because small molecules are rarely

fully  $^{13}\text{C}$  labeled. Even if the molecules were fully labeled, the  $^{13}\text{C}$  through-bond connections usually are obtained directly from other NMR experiments such as HCCCH or indirectly by combining the information from  $^1\text{H}$ - $^1\text{H}$  COSY with  $^{13}\text{C}$ - $^1\text{H}$  HMQC and heteronuclear multiple bond correlation (HMBC)<sup>24</sup> NMR experiments. NMR 2D  $^{13}\text{C}$ - $^{13}\text{C}$  COSY spectral data are similar conceptually to ideas that are used in the first order  $^1\chi$  connectivity indices<sup>25</sup> and the modified adjacency matrix.<sup>26</sup>

In 3D-QSDAR, 2D  $^{13}\text{C}$ - $^{13}\text{C}$  distance spectra that contain short, medium, and long through-space connectivity spectral patterns are produced by using the structurally assigned predicted spectra and selecting a distance range for nucleus to nucleus distance ( $r$ ). This is analogous to 2D  $^1\text{H}$ - $^1\text{H}$  Nuclear Overhauser Effect Spectroscopy (NOESY) NMR experiments where correlations through space are found for neighboring protons that are less than  $5 \text{ \AA}$  away with an off-diagonal cross-peak.<sup>27</sup> The size of the cross-peak in the NOESY experiment is dependent on the distance between the protons, the mixing time of the experiment, and the number of different NOE spin diffusion pathways available for dipolar magnetization transfer.  $^{13}\text{C}$ - $^{13}\text{C}$  NOESY experiments for all practical purposes are never executed again because most small compounds are not fully  $^{13}\text{C}$  labeled.

The binding of steroids to many receptors including to the corticosteroid binding globulin are strongly linked to the structural environment around position 3 and 17 of the steroids.<sup>1-3</sup> In the compressed 3D-connectivity matrix, the modeler can select which 2D spectral-distance range to observe. The distance between position 3 and 17 in a steroid backbone would fall in the long atom-to-atom connections of the 3D-connectivity matrix. The long-range distance was used for these models so that many of the carbons in the A-ring were connected through space to many of the carbon atoms in the D-ring and chains extended off from position 17 in the D-ring. Presently there are no NMR experiments that directly record structural distance information that is greater than  $5 \text{ \AA}$  apart. The distance related topological indices<sup>28</sup> and the 2D  $^{13}\text{C}$ - $^{13}\text{C}$  distance connectivity spectral data are based on similar distance related concepts.

This paper demonstrates that structural information combined with  $^{13}\text{C}$  NMR spectra in the form of through-bond and through spatial distance connectivity information can be used to produce a reliable QSDAR model of steroids binding to the corticosteroid binding globulin.

## PROCEDURES

Figure 1 and Table 1 contain previously reported steroids binding data used for training these models. Compounds in Table 1 had their  $^{13}\text{C}$  NMR spectra simulated using the Advanced Chemistry Developments (ACD) Labs CNMR predictor software, version 4.0.<sup>29</sup> All of the CoSCoSA models were based on predicted  $^{13}\text{C}$  NMR spectra. The use of predicted NMR spectra is not necessary to build the CoSCoSA models, but it saves time and money. Predicted  $^{13}\text{C}$  NMR data allow for the spectra to be independent of the solvent used. The CoSCoSA modeling, LOO cross-validation, and prediction processes were completely computerized.

Figure 2 shows the flowchart on the CoSCoSA modeling procedure. The structures are used to predict 1D  $^{13}\text{C}$  NMR

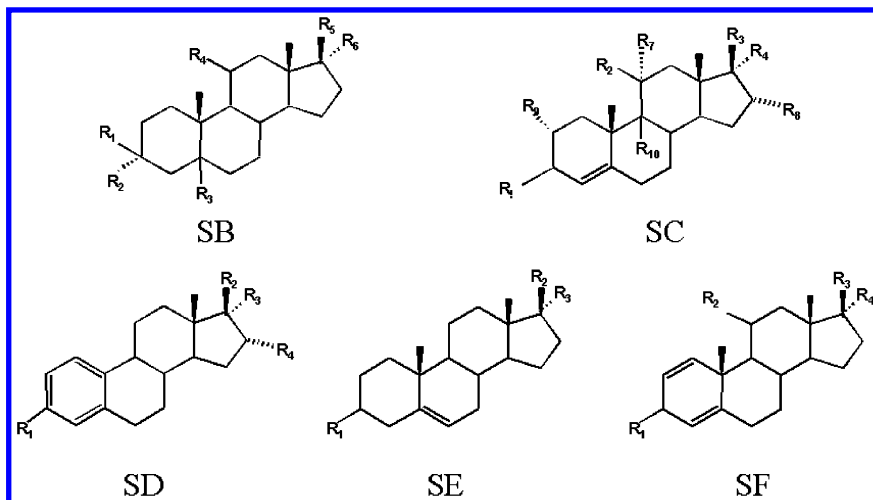


**Figure 1.** Structures SB–SF used with Table 1 for the corticosteroid binding globulin steroid series.

**Table 1.** Structures of Corticosteroids Used in QSDAR Models of Corticosteroid Binding Globulin Data

no.	structure <sup>a</sup>	activity	R <sub>1</sub>	R <sub>2</sub>	R <sub>3</sub>	R <sub>4</sub>	R <sub>5</sub>	R <sub>6</sub>	R <sub>7</sub>	R <sub>8</sub>	R <sub>9</sub>	R <sub>10</sub>
1	SB	5.00	OH	H	H	H	OH	H				
2	SE	5.00	OH	OH	H							
3	SC	5.76	=O	H	=O				H	H	H	H
4	SB	5.61	H	OH	H	H	=O					
5	SC	7.88	=O	OH	COCH <sub>2</sub> OH	H			H	H	H	H
6	SC	7.88	=O	OH	COCH <sub>2</sub> OH	OH			H	H	H	H
7	SC	6.89	=O	=O	COCH <sub>2</sub> OH	OH				H	H	H
8	SE	5.00	OH	=O								
9	SC	7.65	=O	H	COCH <sub>2</sub> OH	H			H	H	H	H
10	SC	7.88	=O	H	COCH <sub>2</sub> OH	OH			H	H	H	H
11	SB	5.92	=O		H	H	OH	H				
12	SD	5.00	OH	OH	H	H						
13	SD	5.00	OH	OH	H	OH						
14	SD	5.00	OH	=O		H						
15	SB	5.23	H	OH	H	H	=O					
16	SE	5.23	OH	COMe	H							
17	SE	5.00	OH	COMe	OH							
18	SC	7.38	=O	H	COMe	H			H	H	H	H
19	SC	7.74	=O	H	COMe	OH			H	H	H	H
20	SC	6.72	=O	H	OH	H			H	H	H	H
21	SF	7.51	=O	OH	COCH <sub>2</sub> OH	OH						
22	SC	7.55	=O	OH	COCH <sub>2</sub> OCOMe				H	H	H	H
23	SC	6.78	=O	=O	COMe	H				H	H	H
24	SC	7.20	=O	H	COCH <sub>2</sub> OH	H			OH	H	H	H
25 <sup>b</sup>	SC	6.14	=O	H	OH	H			H	H	H	H
26	SC	6.25	=O	H	COMe	OH			H	OH	H	H
27	SC	7.12	=O	H	COMe	H			H	Me	H	H
28 <sup>b</sup>	SC	6.82	=O	H	COMe	H			H	H	H	H
29	SC	7.69	=O	OH	COCH <sub>2</sub> OH	OH			H	H	Me	H
30	SC	5.80	=O	OH	COCH <sub>2</sub> OH	OH			H	H	Me	F

<sup>a</sup> Structures according to refs 1, 22, and 23. <sup>b</sup> H (hydrogen) instead of Me at C<sub>10</sub> steroid skeleton.

spectra. The resolution of the 2D spectra was reduced to 2.0 and 3.0 ppm in both dimensions to populate many of the NMR bins for statistical analysis and reduce the effects of uncertainties in the simulated spectra. The spectral widths were chosen because of convenience. The 2D <sup>13</sup>C-<sup>13</sup>C NMR spectra were saved as two-dimensional bins under the peak within a certain spectral range and normalized to an integer. A single carbon-to-carbon connectivity was assigned an area of 100, two carbon-to-carbon connections in a bin had an area of 200, and so forth. This was done so that all the carbon-to-carbon connections would have a similar signal-to-noise ratio.

The predicted NMR spectra were calculated by a substructure similarity technique called HOSE,<sup>30</sup> which correlates similar structures with similar NMR chemical shifts.

Therefore, the errors produced in the simulated NMR spectra were propagated through the similar structures found in the training set of the QSDAR models. This conveniently reduced the effective error when using the training set to predict unknown sample affinities for compound spectra predicted using the same HOSE routine.

The structurally assigned <sup>13</sup>C NMR spectra were used to produce predicted 2D <sup>13</sup>C-<sup>13</sup>C COSY and theoretical 2D <sup>13</sup>C-<sup>13</sup>C distance spectra. The arrows in Figure 3A show the through-bond neighboring carbon-to-carbon connections of a steroid backbone molecule without any side chains. These through-bond carbon-to-carbon connections were used to simulate a 2D <sup>13</sup>C-<sup>13</sup>C COSY spectrum of the steroid compounds. The arrows in Figure 3B show the through-space carbon-to-carbon connections that are greater than 6.9 Å apart

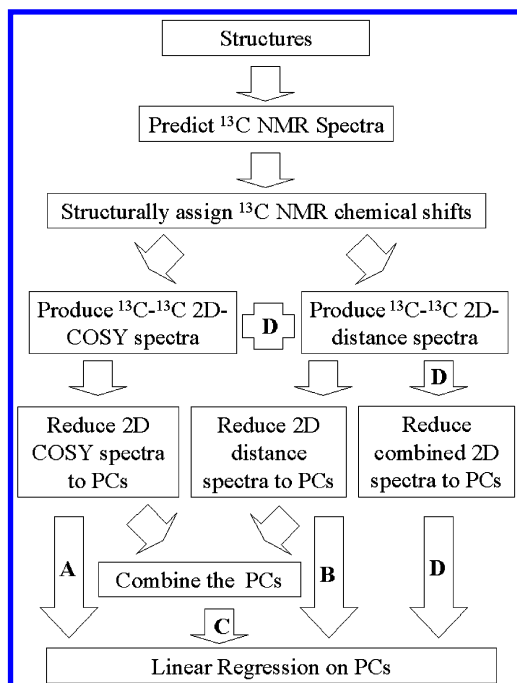


**Figure 2.** The procedural flowchart for CoSCoSA modeling. (A) The  $^{13}\text{C}$ - $^{13}\text{C}$  COSY data. (B) The  $^{13}\text{C}$ - $^{13}\text{C}$  distance connectivity data greater than 6.9 Å. (C) The combined  $^{13}\text{C}$ - $^{13}\text{C}$  COSY and  $^{13}\text{C}$ - $^{13}\text{C}$  distance connectivity PCs. (D) The combined  $^{13}\text{C}$ - $^{13}\text{C}$  COSY and  $^{13}\text{C}$ - $^{13}\text{C}$  distance connectivity data before PCs are extracted from the combined data.

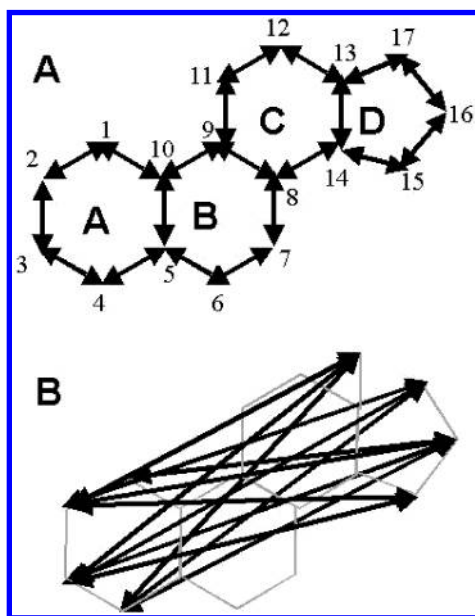


**Figure 3.** (A) The arrows represent the carbon to carbon through nearest neighbor bond connections for the backbone of a steroid used in the predicted 2D  $^{13}\text{C}$ - $^{13}\text{C}$  COSY spectra. (B) The arrows represent the carbon to carbon through spatial distance connections used in the theoretical 2D  $^{13}\text{C}$ - $^{13}\text{C}$  distance spectra.

in a steroid backbone without any side chains. These through-space carbon-to-carbon connections and any other through-space carbon-to-carbon distance connections that were greater than 6.9 Å were used to produce a theoretical 2D  $^{13}\text{C}$ - $^{13}\text{C}$  distance connectivity spectra that had cross-peaks when two carbons were greater than 6.9 Å apart. The 2D  $^{13}\text{C}$ - $^{13}\text{C}$  COSY and 2D  $^{13}\text{C}$ - $^{13}\text{C}$  distance connectivity spectra are symmetrical across the diagonal, and for modeling purposes only half of each individual spectrum was used. The 1D  $^{13}\text{C}$  NMR spectra

in these CoSCoSA models were not used because the 1D chemical shifts do not provide any new information.

Four CoSCoSA models of binding to the corticosteroid binding globulin can be built from the 2D COSY and 2D long-range distance spectra. One model can be made from the 2D COSY spectra, and one model can be developed using the 2D long-range distance spectra. COSY and distance spectra were combined in two different ways, using the combined spectra (3D) or using the combined principal components (PCs) from the COSY PCs and Distance PCs. In Figure 2 arrow A represents the 2D  $^{13}\text{C}$ - $^{13}\text{C}$  COSY spectra data that were reduced to PCs. These PCs were then used for multiple linear regression to produce a model for the 2D  $^{13}\text{C}$ - $^{13}\text{C}$  COSY data. In Figure 2, arrow B represents the 2D  $^{13}\text{C}$ - $^{13}\text{C}$  distance connectivity data that were reduced to PCs. These PCs were then used for multiple linear regression to produce a model for the 2D  $^{13}\text{C}$ - $^{13}\text{C}$  distance connectivity data. In Figure 2 arrow C represents the procedure that used the combined PCs from the 2D  $^{13}\text{C}$ - $^{13}\text{C}$  COSY (arrow A) and the 2D  $^{13}\text{C}$ - $^{13}\text{C}$  distance connectivity (arrow B) to produce a combined through bond and through space CoSCoSA model. In Figure 2 arrow D represents the procedure that used the combined 2D  $^{13}\text{C}$ - $^{13}\text{C}$  COSY and the 2D  $^{13}\text{C}$ - $^{13}\text{C}$  distance connectivity spectral data that were then reduced to PCs. These PCs were then used for multiple linear regression to produce a model for the three-dimensional representation of the 2D  $^{13}\text{C}$ - $^{13}\text{C}$  COSY and 2D  $^{13}\text{C}$ - $^{13}\text{C}$  distance spectra data.

All principal component linear regression statistical analyses were performed by Statsoft Statistica software version 5.5 or 6.0.<sup>31</sup> The CoSCoSA QSDAR models were produced in which the connectivity bins were evaluated with forward multiple linear regression analysis using only the most correlated PCs from both the 2D  $^{13}\text{C}$ - $^{13}\text{C}$  COSY and 2D  $^{13}\text{C}$ - $^{13}\text{C}$  distance connectivity spectra. The F-test for many of the models continued to rise until the number of components in the model equalled the number of compounds in the training set. This is why the number of PCs used in the CoSCoSA models was limited to 3 and 8.

The analysis of each PCR CoSCoSA model was done by the LOO cross-validation procedure where each compound is systematically excluded from the training set and its binding activity is predicted by the model.<sup>32</sup> The cross-validated  $r^2$  (termed  $q^2$ ) can be derived from  $q^2 = 1 - (\text{PRESS})/\text{SD}$ . Where PRESS is the sum of the differences between the actual and predicted activity data for each molecule during LOO cross-validation, and SD is the sum of the squared deviations between the measured and mean activities of each molecule in the training set. We believe that  $q^2$  is a more valid measure than  $r^2$  for assessing the reliability of a mathematical model intended for predictive applications.

Another model for predicting steroid binding activity to the corticosteroid binding globulin was developed using a parallel distributed-artificial neural network (PD-ANN). The PD-ANN is an algorithm that allows for simultaneous training and testing of multiple neural networks. The drawback to using an ANN has been the time required finding an optimal network configuration. Traditionally this search has been performed in serial fashion, one configuration at a time, on one computer at a time. The PD-ANN simply takes advantage of an Internet based parallel distribution scheme to perform the optimization task on multiple



machines simultaneously. The result is a dramatic decrease in the time required for finding an optimal network configuration. For this study, the artificial neural network consisted of an error back-propagating, feed forward Java code. The back-propagation algorithm in the PD-ANN is based on Rummelhart, Hinton, and Williams' generalized delta rule.<sup>33</sup> It was developed "in house" and parallel distributed using JGravity, a Java-based parallel distribution platform.<sup>34</sup> We are participating in the beta test phase of JGravity development.

The PD-ANN receives raw data broken into bins with the population in each bin assigned to its own input node. These nodes are interconnected to a "hidden layer" containing a number of processing elements called hidden nodes. The hidden layer is finally interconnected to the output layer. The training of each neural network in the PD-ANN consists of repeated cycles of presenting examples to the input nodes while simultaneously presenting corresponding output examples to the output node. The back-propagation code adjusts weights between the input, hidden, and output layer connections using a gradient descent least squares technique to reduce the error between the net predicted output and the actual output on which it is training. Training stops when the error between the actual output values and the net-produced output values drops below a predetermined threshold value.

In this study, spectral data were read into each network through the input nodes and passed through one hidden layer that was connected to an output layer. Thus the neural network architecture consisted of three fully connected layers. A 593 node input layer was connected to a hidden layer, which was then connected to a one node output layer. The 593 nodes of the input layer corresponded to the number of occupied 2D COSY and 2D long-range distance spectral bins. Transfer functions were used within the back-propagation algorithm to calculate the values of the hidden and output nodes. The one node of the output layer corresponded to the binding activity for each molecule.

The parallel distributed network algorithm was used to optimize the neural network configuration. Optimization refers to the search of the multidimensional space created by the adjustable parameters of the back-propagation code to find the network configuration that provides the best prediction of binding affinity based on spectral data. The algorithm, which resided on a central computer, distributed neural networks with different configurations in parallel to four personal computers. The impacts of varying permutations and combinations of the number of hidden nodes, the number of (back-propagation) cycles, the transfer functions (sigmoid, hyperbolic tan, or arc tan), and the learning rate were evaluated based on each one's cross-validation results at benchmark cycles during the back-propagation process. Validation or testing of each configuration was performed on each participating computer node, and only the results were returned to the central computer.

The algorithm on each computer node removed a small number of examples from the training set for testing. Each network then trained to the specified number of cycles on the somewhat abridged set using the parameters assigned by the central computer. When training was completed, the removed data was propagated through the trained network and predictions were obtained, the quality of which was

subject to validation. On each participating computer node, this process of removing data, training the network, and propagating the removed data was repeated by the algorithm with each network configuration, until all of the training set samples were used to test the network. At that time the master computer assigned a new configuration for the node computer to work on. This assignment and reassignment process was repeated on all the available computer nodes until the master computer finished its task list. The task list is a user-specified list of all the test configurations.

More than 100 varying network configurations were evaluated over a couple of days using four high-speed Pentium personal computers. Two types of cross-validations were performed. In one case each distributed neural network removed three examples and trained on the rest, rotating through the rest of the data on subsequent training sessions, and thus performing a comprehensive series of leave-three-out cross-validations. In another case 10 examples were left out, performing a leave-ten-out cross-validation.

The configuration consisting of 593 input, 198 hidden, and 1 output nodes provided the best validated results. This roughly corresponds to a hidden layer that is equal to  $1/3n$ , where  $n$  = number of input nodes. This is a common input-hidden node relationship for three layer feed forward networks, and for many backprop ANN problems, it often is an optimal configuration.<sup>35</sup> However, due to the large number of input nodes, this configuration leads to a substantial number of interconnections between the input, hidden, and output nodes (since all of the nodes are interconnected). This could have been a problem since it is well-known in ANN applications that the greater the number of interconnections, the easier the ANN learns its training set, but also the worse it predicts unknowns.<sup>36</sup> This would have defeated the purpose of this application, since the intention of this study was to construct a model that provides good cross-validated predictions of biological activity, not to memorize the training data. However, due to the PD-ANNs rapid turn around time for obtaining cross-validated results, it was quickly realized that the configuration generalized well and provided high quality cross-validated results.

The best results were obtained when the network was trained for 3400 cycles, with a learning rate of 0.1, and using a sigmoid transfer function. Use of a sigmoid transfer function in the back-propagation algorithm required that the data (input and output) be scaled within a range between 0 and 1. The raw data for this model was actually scaled from 0.1 to 0.9.

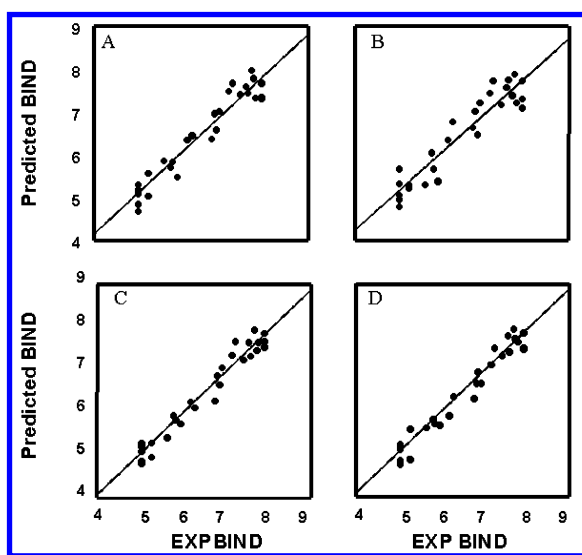
## RESULTS

Table 2 contains a comparison of the model performance parameters  $n$ ,  $r^2$ ,  $q^2$ , and number of components for the QSAR,<sup>2</sup> HE-state/E-state,<sup>3</sup> E-state,<sup>3</sup> SOM,<sup>4</sup> combination QSAR/E-state,<sup>5</sup> 2D CoSASA,<sup>6</sup> 1D CoSA,<sup>6</sup> 4 CoSCoSA, and 2 CoSCoSA PD-ANN models. We did not use the compound aldosterone because it has two structural conformations, and therefore our comparisons to previous models<sup>2-5</sup> have one less compound in the training set. All four CoSCoSA models with eight PCs have a strong correlation ( $r^2$ ) and cross-validated variance ( $q^2$ ) and are favorable when compared to the previous published models of binding to the corticosteroid binding globulin.

**Table 2.** Model Performance Parameters  $N$ ,  $r^2$ ,  $q^2$ , and Number of Components

model	n	$r^2$	$q^2$	components
QSAR (2)	31	0.72	0.68 <sup>a</sup>	3 (PCs)
HE state/E-state (3)	31	0.98 <sup>a</sup> /0.96 <sup>b</sup>	0.80 <sup>a</sup> /0.76 <sup>b</sup>	3 <sup>a</sup> (PCs)/5 <sup>b</sup> (PCs)
E-state (3)	31	0.96 <sup>a</sup> /0.96 <sup>b</sup>	0.79 <sup>a</sup> /0.67 <sup>b</sup>	3 <sup>a</sup> (PCs)/4 <sup>b</sup> (PCs)
SOM (4)	31	0.85	—	3 (PCs)
QSAR/E-state (5)	30	0.82	0.78	3 (atoms)
2D CoSASA (6)	30	0.80	0.73	3 (atoms)
1D CoSA (6)	30	0.80	0.78	3 (bins)
CoSCoSA (COSY)	30	0.84/0.93	0.74/0.88	3 (PCs)/8 (PCs)
CoSCoSA (distance)	30	0.66/0.89	0.38/0.79	3 (PCs)/8 (PCs)
CoSCoSA (COSY + distance)	30	0.84/0.96	0.74/0.92	3 (PCs)/8 (PCs)
CoSCoSA (3D <sup>c</sup> )	30	0.78/0.92	0.68/0.81	3 (PCs)/8 (PCs)
CoSCoSA-PD-ANN (3D <sup>c</sup> )	30	0.96	0.78 <sup>d</sup>	593:198:1
CoSCoSA-PD-ANN (3D <sup>c</sup> )	30	0.96	0.73 <sup>e</sup>	593:198:1

<sup>a</sup> 1.0 Å models. <sup>b</sup> 2.0 Å models. <sup>c</sup> 3D is the combination of COSY and distance data before PC extraction. <sup>d</sup> A leave-three-out  $q_3^2$ . <sup>e</sup> A leave-ten-out  $q_{10}^2$ .



**Figure 4.** Plot of the predicted binding versus experimental binding. (A) The  $^{13}\text{C}$ - $^{13}\text{C}$  COSY data. (B) All the  $^{13}\text{C}$ - $^{13}\text{C}$  distance connectivity data greater than 6.9 Å. (C) The combined  $^{13}\text{C}$ - $^{13}\text{C}$  COSY and  $^{13}\text{C}$ - $^{13}\text{C}$  distance connectivity PCs. (D) The combined  $^{13}\text{C}$ - $^{13}\text{C}$  COSY and  $^{13}\text{C}$ - $^{13}\text{C}$  distance connectivity data before PCs are extracted from the combined data.

Figure 4A is a plot of the predicted binding versus experimental binding for the CoSCoSA 2.0 ppm resolution model based on  $^{13}\text{C}$ - $^{13}\text{C}$  COSY data. A model based on eight PCs had an explained correlation ( $r^2$ ) of 0.93 and a cross-validated variance ( $q^2$ ) of 0.88, which indicates self-consistency and excellent predictive capability. Figure 4B is a plot of the predicted binding versus experimental binding for the CoSCoSA 2.0 ppm resolution model based on  $^{13}\text{C}$ - $^{13}\text{C}$  distance greater than 6.9 Angstroms data. Using eight PCs the explained correlation ( $r^2$ ) of this model is 0.89 and the cross-validated variance ( $q^2$ ) is 0.79. Figure 4C is a plot of the predicted binding versus experimental binding for the CoSCoSA 2.0 ppm resolution model based on the combined  $^{13}\text{C}$ - $^{13}\text{C}$  COSY and  $^{13}\text{C}$ - $^{13}\text{C}$  distance connectivity PCs. The explained correlation ( $r^2$ ) of this model is 0.96, and the cross-validated variance ( $q^2$ ) of this model is 0.92, which indicates excellent predictive capability. Figure 4D is a plot of the predicted binding versus experimental binding for the CoSCoSA 2.0 ppm resolution model based on the combined  $^{13}\text{C}$ - $^{13}\text{C}$  COSY and  $^{13}\text{C}$ - $^{13}\text{C}$  distance connectivity spectral data before principal component extraction. The explained cor-

relation ( $r^2$ ) of this model is 0.92, and the cross-validated variance ( $q^2$ ) is 0.81.

All of the spectral bins based on the combination of  $^{13}\text{C}$ - $^{13}\text{C}$  COSY and  $^{13}\text{C}$ - $^{13}\text{C}$  distance spectra were used to develop the CoSCoSA PD-ANN model. The explained correlation ( $r^2$ ) of this model is 0.96. Two cross-validated variance coefficients were calculated for this model. The leave-three-out ( $q_3^2$ ) procedure yielded a value of 0.78, and the leave-ten-out ( $q_{10}^2$ ) procedure yielded a value of 0.73. These numbers illustrate a high degree of consistency and predictive capability for the PD-ANN model.

## DISCUSSION

All four CoSCoSA models based on eight PCs have a  $q^2$  greater than the 0.68 seen for the QSAR model. Three of the four CoSCoSA models based on three PCs have a  $q^2$  greater than the 0.68. The only CoSCoSA model that did not have a  $q^2$  greater than 0.68 was the  $^{13}\text{C}$ - $^{13}\text{C}$  distance connectivity model based on only three PCs. The HE-state and E-state models have a greater  $r^2$  than all the QSDAR models, but these models are very computational-intensive with many distance formulas used for every point in the grid. Still, all the 2.0 ppm resolution CoSCoSA models based on eight PCs have explained variance ( $r^2$ ) greater than 0.89 and a cross-validated variance ( $q^2$ ) greater than 0.79. All the CoSCoSA models with eight PCs have a predictability that are much better or comparable to the predictability for QSAR, CoSA, CoSASA, HE-state/E-state, and E-state models. The reason we are comparing models based on eight PCs to models based on three or four components is that these COSCOSA models are “digital” in nature and the other QSAR, HE-states, and E-states models are in “analog” format. Digital information needs more components to present the same information (10 binary components to represent a number less than 999) as analogue electronics (three variable components to represent a number less than 999), but the resulting information is presented with a higher signal-to-noise value. Our CoSCoSA models see essentially the same thing, although these models are displaying the same electrostatic information that is used in QSAR or E-states models. CoSCoSA models have a better signal-to-noise (predictability) than other models when more components are used.

Another explanation for the fact that the cross-validated variance of the CoSCoSA model was as good as the other

models is that even simulated NMR spectral data are more accurate than the errors introduced by solvent effects, partial charges, dielectrics, and structural conformations used during the calculation of electrostatic potentials. All of the assumptions and approximations are prone to produce significant error.  $^{13}\text{C}$  NMR spectral data takes into account all structural conformations and complete solvent effects to produce a "quantum mechanical energy" that represents the average structural environment for every carbon atom in the molecule.

In our earlier CoSA QSDAR model started with only 256 spectral bins, a number then reduced to 94 spectral bins when all the columns with only zeroes or with only one nonzero entry were removed. In our 2.0 ppm CoSCoSA models, we started with 6441 two-dimensional bins, a number then reduced to 271 for the  $^{13}\text{C}$ - $^{13}\text{C}$  COSY data and 322 for the  $^{13}\text{C}$ - $^{13}\text{C}$  distance connectivity data when all the columns with only zeroes were removed. The models used less than 5% of the available 2D connectivity spectral space with this training set and a 2 ppm resolution bin size.

To understand the effect of combining all bins with only one "hit" in the bin to the nearest bin with a "hit". When multiple bins with "hits" were equally close to the bin with one "hit", the one "hit" bin was moved to the bin with the least number of "hits". When all the bins with one "hit" were removed, the 2 ppm  $^{13}\text{C}$ - $^{13}\text{C}$  COSY had 93 of the 271 bins removed and the 2 ppm  $^{13}\text{C}$ - $^{13}\text{C}$  distance connectivity data had 128 of the 322 bins removed. Using the new  $^{13}\text{C}$ - $^{13}\text{C}$  COSY data with no bins with only one "hit" in a bin for a model the  $r^2$  increased from 0.93 to 0.94 and  $q^2$  increased from 0.88 to 0.89. The reduced  $^{13}\text{C}$ - $^{13}\text{C}$  distance connectivity data produced a model where the  $r^2$  increased from 0.89 to 0.91 and  $q^2$  increased from 0.79 to 0.81. Using both the reduced  $^{13}\text{C}$ - $^{13}\text{C}$  COSY and  $^{13}\text{C}$ - $^{13}\text{C}$  distance connectivity PCs for a model, the  $r^2$  decreased from 0.96 to 0.95 and  $q^2$  decreased from 0.92 to 0.90. Using both new  $^{13}\text{C}$ - $^{13}\text{C}$  COSY and  $^{13}\text{C}$ - $^{13}\text{C}$  distance connectivity combined data before the extraction of PCs the  $r^2$  increased from 0.92 to 0.93 and  $q^2$  increased from 0.81 to 0.84.

We wanted to determine the effect of increasing the bin size to 3.0 ppm. In our 3.0 ppm CoSCoSA models we started with 2926 two-dimensional bins, a number then reduced to 199 for the  $^{13}\text{C}$ - $^{13}\text{C}$  COSY data and 253 for the  $^{13}\text{C}$ - $^{13}\text{C}$  distance connectivity data when all the columns with only zeroes were removed. For the model based on  $^{13}\text{C}$ - $^{13}\text{C}$  COSY data, the  $r^2$  decreased from 0.93 to 0.87 and  $q^2$  decreased from 0.88 to 0.79. For the model based on  $^{13}\text{C}$ - $^{13}\text{C}$  distance connectivity data, the  $r^2$  increased from 0.89 to 0.90 and  $q^2$  decreased from 0.79 to 0.74. For the model based on the combined  $^{13}\text{C}$ - $^{13}\text{C}$  COSY and  $^{13}\text{C}$ - $^{13}\text{C}$  distance connectivity PCs, the  $r^2$  decreased from 0.96 to 0.89 and  $q^2$  decreased from 0.96 to 0.80. For the model based on the combined  $^{13}\text{C}$ - $^{13}\text{C}$  COSY and  $^{13}\text{C}$ - $^{13}\text{C}$  distance connectivity data before extraction of principal components, the  $r^2$  was unchanged at 0.92 and  $q^2$  increased from 0.81 to 0.84.

We wanted to determine the effect of using different distance cutoff for the  $^{13}\text{C}$ - $^{13}\text{C}$  distance connectivity spectral CoSCoSA models. Instead of using all distance connections greater than 6.9 Å we used the same set of atom to atom distance for all the compounds. This meant using the distance connectivity set from the smallest compounds (no chains off of the steroids) for all the compounds. The smallest compounds had 26 distance connectivity interactions greater

than 6.9 Å, 13 on each side of the 2D  $^{13}\text{C}$ - $^{13}\text{C}$  long-range distance spectra. When using all distance connection interactions greater than 6.9 Å, the number of interactions varied for each compound. When we used only this new  $^{13}\text{C}$ - $^{13}\text{C}$  distance connection spectra data with 13 interactions for each compound to build a CoSCoSA model, the  $r^2$  of 0.89 did not change and the  $q^2$  decreased from 0.79 to 0.72. When we used the new  $^{13}\text{C}$ - $^{13}\text{C}$  distance connectivity PCs based on the same 13 distance connections for each steroid compound with the original  $^{13}\text{C}$ - $^{13}\text{C}$  COSY PCs to build a new CoSCoSA model, the  $r^2$  decreased from 0.96 to 0.95 and the  $q^2$  decreased from 0.92 to 0.89. Using the original  $^{13}\text{C}$ - $^{13}\text{C}$  COSY and the new  $^{13}\text{C}$ - $^{13}\text{C}$  distance connectivity combined data before the extraction of PCs the  $r^2$  increased from 0.92 to 0.95 and  $q^2$  increased from 0.81 to 0.93.

It is interesting to note that a strong predictive model was produced by the PD-ANN using the combined COSY and distance  $^{13}\text{C}$  spectral data. There was no preprocessing (such as principal components or other types of regression analysis to extract features) performed on the data prior to its use. This model used the raw spectral information. The strength of the model is clearly demonstrated with the  $q_{10}^2$  of 0.73. The total data set consisted of only 30 compounds. Thus each time 10 compounds were left out, the data set used to build the model was depleted by 33%.

The CoSCoSA models takes into account the average uncertainty in the predicted  $^{13}\text{C}$  NMR data. It therefore reduces the information content of the spectrum by reducing the number of spectral bins and losing the shape of the chemical shift peak. Still, the CoSCoSA models retained enough information by increasing the number of chemical shifts in many spectral bins to produce reliable models of binding to the corticosteroid binding globulin. The NMR chemical shift peak has information about atom adjacency, solvent effects, and average structural conformation, but the shape of the peak is greatly affected by shimming and temperature-dependent dynamics. We lose the information about the shape of the peak when we use bin sizes greater than the average peak width, as is the case for this study.

## DISCUSSION

Structure and chemical shift information from the 3D-connectivity matrix was used to produce very accurate models of steroids binding to the corticosteroid binding globulin. The 3D-connectivity matrix uniquely combines quantum mechanical information from the chemical shifts with nearest neighbor and internal distance connectivity information. The combined information from COSY and long-range distance connectivity information from the 3D-connectivity matrix was able to produce CoSCoSA models that are much more accurate and reliable than QSAR or E-state models based on separate calculations for electrostatics and steric interactions. The cross-validated variance of CoSCoSA models based on simulated  $^{13}\text{C}$  NMR data should improve as the errors introduced by the simulation of the  $^{13}\text{C}$  NMR data are further reduced by improved spectral simulation programs.

The 2D  $^{13}\text{C}$ - $^{13}\text{C}$  COSY nearest neighbor connectivity spectral data should be important for almost any molecular property or binding affinity. In our CoSCoSA models the 2D  $^{13}\text{C}$ - $^{13}\text{C}$  COSY had a higher  $r^2$  and  $q^2$  than the  $^{13}\text{C}$ - $^{13}\text{C}$



distance connectivity data. The  $^{13}\text{C}$ - $^{13}\text{C}$  distance connectivity data will be important when one or more distance-related structural features are required for molecular binding to a receptor. This is the case for steroids binding to the corticosterone binding globulin because regions around position 3 and 17 of the steroid are important for binding.

The CoSCoSA models that combined the  $^{13}\text{C}$ - $^{13}\text{C}$  COSY and  $^{13}\text{C}$ - $^{13}\text{C}$  distance connectivity PCs together produced the models with the highest  $r^2$  and  $q^2$ . The combined  $^{13}\text{C}$ - $^{13}\text{C}$  COSY and  $^{13}\text{C}$ - $^{13}\text{C}$  distance connectivity PCs models were better than the 3D CoSCoSA models because there were twice as many PCs available to build a model with the separated 2D spectral connectivity data.

In CoSCoSA modeling the number and size of bins is very important. Too large a bin size inappropriately lumps distinct spectral information into the same category and too small a bin size suffers from false distinctions based on reduced average bin occupancy values that adversely affect the statistics needed to identify and confirm the pattern. If one uses a huge number of bins, the results will be a model with excellent  $r^2$  and pitiful  $q^2$ ,<sup>37</sup> experimentally without an exhaustive search we have found that 2 and 3 ppm bins seem to work best.

Our investigations showed that the 2 ppm resolution bin seem to work better for the COSY data and the 3 ppm resolution bin seem to work slightly better for the distance connectivity data. This makes sense because there were more COSY nearest neighbor connections than distance connections per molecule and therefore a lower bin size could be used for the COSY data and still produce reliable statistical models. The investigation into moving all the bins with one "hit" in them to the nearest bin with a "hit" had an  $r^2$  and a  $q^2$  that were only slightly improved over the original 2 ppm resolution CoSCoSA models. Changing the cutoffs distance from any distance over 6.9 Å to only the same 13 distance connections from the smallest molecules produced only very small changes in  $r^2$  and  $q^2$ .

The EVA infrared spectral<sup>38</sup> descriptors saw a similar fall off for  $q^2$  when the size of the bin became too large. IR descriptors are similar to NMR descriptors in that they are the eigenvalues energies to the quantum mechanics Schrödinger's equation, but NMR descriptors are easily identified with one atomic nucleus whereas IR descriptors are not identified to one atom.

Future improvements to the CoSCoSA modeling method include the use of other spectra besides  $^{13}\text{C}$  NMR. The most promising NMR spectra is  $^{15}\text{N}$  because it is in many organic molecules. Other NMR spectra that could be used are  $^1\text{H}$ ,  $^{17}\text{O}$ ,  $^{19}\text{F}$ ,  $^{31}\text{P}$  and others depending on the endpoint and training set. Another major improvement will be the use of multiple structures so flexible compounds can be modeled. A 4D-connectivity matrix can be made as a sum of 100 3D-connectivity matrices. In the 4D-connectivity matrix the chemical shifts of atom  $i$  and atom  $j$  will not change, but the distance between atom  $i$  and atom  $j$  will fluctuate. A score of 100 in a 4D-connectivity matrix will represent unvarying distances between two atoms as seen in bonds and very rigid molecules. For flexible molecules there will be a distribution of distance hits along the  $z$ -axis varying from 1 to some maximum. The distributions will be Gaussian, skewed-Gaussian shaped when there is one maximum

distance. When there is more than one maximum other distribution shapes will be seen.

## CONCLUSION

In this paper, there was no attempt to optimize the size of the two-dimensional bins or the distance cutoffs used in the  $^{13}\text{C}$ - $^{13}\text{C}$  2D distance spectra. In any event, accurate CoSCoSA models of steroid compounds binding to corticosteroid binding globulin were developed without having to use an optimization procedure for the bin size and distance connectivity cutoffs. CoSCoSA modeling is a high powered modeling technique because it uniquely combines the quantum mechanics information from the chemical shifts with internal molecular distances. Since we only used 5% of the available 2D chemical shift "space", we believe that we can use this procedure to effectively build reliable models of very large set of noncongeners for a specific endpoint. Optimizing the bin size, the distance cutoffs, multiple structures, multiple spectra, and the number of distance connectivity spectra used in a CoSCoSA model may be needed in looking at other biological, physical, chemical, ADME, and toxicological endpoints.

## REFERENCES AND NOTES

- (1) Mickelson, K. E.; Forsthofel, J.; Westphal, U. Steroid-protein interactions. Human corticosteroid binding globulin: Some physicochemical properties and binding specificity. *Biochemistry* **1981**, *20*, 6211–6218.
- (2) Good, A. C.; So, S.-S.; Richards, W. G. Structure-activity relationships from molecular similarity matrices. *J. Med. Chem.* **1993**, *36*, 433–438.
- (3) Kellogg, G. E.; Kier, L. B.; Gaillard, P.; Hall, L. H. E-state fields: Applications to 3D QSAR. *J. Comput.-Aided Mol. Design.* **1996**, *10*, 513–520.
- (4) Polanski, J. The receptor-like neural network for modeling corticosteroid and testosterone binding globulins. *J. Chem. Inf. Comput. Sci.* **1997**, *37*, 553–561.
- (5) De Gregorio, C.; Kier, L. B.; Hall, L. H. QSAR modeling with electrotopological state indices: Corticosteroids. *J. Comput.-Aided Mol. Design.* **1988**, *2*, 557–561.
- (6) Beger, R.; Wilkes, J. Developing  $^{13}\text{C}$  NMR quantitative spectrometric data-activity relationship (QSDAR) models of steroid binding to the corticosteroid binding globulin. *J. Comput.-Aided Mol. Design.* **2001**, *15*, 659–669.
- (7) Beger, R. D.; Wilkes, J. G.  $^{13}\text{C}$  NMR quantitative spectrometric data-activity relationship (QSDAR) models to the aromatase enzyme. *J. Chem. Inf. Comput. Sci.* **2001**, *41*, 1360–1366.
- (8) Beger, R. D.; Wilkes, J. G. Models of polychlorinated dibenzodioxins, dibenzofurans, and biphenyls binding affinity to the aryl hydrocarbon receptor developed using  $^{13}\text{C}$  NMR data. *J. Chem. Inf. Comput. Sci.* **2001**, *41*, 1322–1329.
- (9) Katritzky, A. R.; Ignatchenko, E. S.; Barcock, R. A.; Lobanov, V. S. Prediction of gas chromatographic retention times and response factors using a general quantitative structure-property relationship. *Anal. Chem.* **1994**, *66*, 1799–1807.
- (10) Katritzky, A. R.; Mu, L.; Lobanov, V. S.; Karelson, M. Correlation of boiling points with molecular structure. 1. A training set of 298 diverse organics and a test set of 9 simple inorganics. *J. Phys. Chem.* **1996**, *100*, 10400–10407.
- (11) Fujita, T.; Iwasa, J.; Hansch, C. A new substituent constant,  $\pi$ , derived from partition coefficient. *J. Am. Chem. Soc.* **1964**, *86*, 5175–5180.
- (12) Branbury, S. P. Quantitative structure-activity relationship and ecological risk assessment: An overview of predictive aquatic toxicology research. *Toxicology* **1995**, *25*, 67–89.
- (13) Cramer, R. D.; Paterson, D. E.; Bunce, J. D. Comparative molecular field analysis (CoMFA). 1. Effect of shape on binding of steroids to carrier proteins. *J. Am. Chem. Soc.* **1988**, *110*, 5959–5967.
- (14) Beger, R. D.; Bolton, P. H. Protein  $\phi$  and  $\psi$  dihedral restraints determined from multidimensional hypersurface correlations of backbone chemical shifts and their use in the determination of protein tertiary structures. *J. Biomol. NMR*, **1997**, *10*, 129–142.
- (15) Wishart, D. S.; Sykes, B. D. Chemical shifts as a tool for structure determination. *Methods Enzymol.* **1994**, *239*, 363–392.



- (16) Kvasnicka, V. An application of neural networks in chemistry. Prediction of  $^{13}\text{C}$  NMR chemical shifts. *J. Math. Chem.* **1991**, 6, 63–76.
- (17) Emsley, J. W.; Feeney, J.; Sutcliffe, L. H. *High-Resolution Nuclear Magnetic Resonance*; Pergamon Press Ltd.: Oxford, 1965; Vol. I, Chapter 8, p 287.
- (18) Hansch, C.; Leo, A. *Exploring QSAR – Fundamentals and applications in chemistry and biology*; The American Chemical Society: Washington, DC, 1995.
- (19) Klopman, G. Artificial intelligence approach to structure–activity studies. Computer automated structure evaluation of biological activity of organic molecules. *J. Am. Chem. Soc.* **1984**, 106, 7315–7321.
- (20) Klopman, G. MULTICASE1. A hierarchical computer automated structure evaluation program. *Quant. Struct. Act. Relat.* **1992**, 11, 176–184.
- (21) Aue, W. P.; Bartholdi, E.; Ernst, R. R. Two-dimensional spectroscopy. Application to nuclear magnetic resonance. *J. Chem. Phys.* **1976**, 64, 2229–2246.
- (22) Bodenhausen, G.; Ruben, D. J. Natural abundance nitrogen-15 NMR by enhanced heteronuclear spectroscopy. *Chem. Phys. Lett.* **1980**, 69, 185–189.
- (23) Bax, A.; Griffey, R. H.; Hawkins, B. L. Sensitivity-enhanced correlation of  $^{15}\text{N}$  and  $^1\text{H}$  chemical shifts in natural-abundance samples via multiple quantum coherence. *J. Am. Chem. Soc.* **1983**, 105, 7188–7190.
- (24) Bax, A.; Summers, M. F.  $^1\text{H}$  and  $^{13}\text{C}$  Assignments from sensitivity-enhanced detection of heteronuclear multiple-bond connectivity by 2D multiple quantum NMR. *J. Am. Chem. Soc.* **1986**, 108, 2093–2094.
- (25) Randić, M. On the characterization of molecular branching. *J. Am. Chem. Soc.* **1975**, 97, 6609–6615.
- (26) Burden, F. R. A chemically intuitive molecular index based on eigenvalues of a modified adjacency matrix. *Quant. Struct.-Act. Relat.* **1997**, 16, 309–314.
- (27) Kumar, A.; Ernst, R. R.; Wuthrich, K. A two-dimensional nuclear Overhauser enhancement (2D NOE) experiment for the elucidation of complete proton–proton cross-relaxation networks in biological macromolecules. *Biochem. Biophys. Res. Comms.* **1980**, 95, 1–6.
- (28) Balaban, A. T. Highly discriminating distance based topological index. *Chem. Phys. Lett.* **1982**, 89, 399–404.
- (29) CNMR predictor, ACD/Labs Toronto, Canada, 2000.
- (30) Bremser, W. HOSE – a Novel substructure Code. *Anal. Chim. Acta* **1978**, 103, 355–365.
- (31) Statistica, version 6.0, StatSoft, Tulsa, OK, 2001.
- (32) Cramer, R. D.; Bunce, J. D.; Patterson, D. E. Cross-validation, bootstrapping, and partial least squares compared with multiple regression in conventional QSAR studies. *Quant. Struct.-Act. Relat.* **1988**, 7, 18–25.
- (33) Jgravity, version 1.0 beta-1 build-10, Titan Systems Corporation/LinCom Division.
- (34) Rumelhart, D. E.; McClelland, T. L. *Parallel Distributed Processing*; Brandford Books/MIT Press: Cambridge, MA, 1986.
- (35) Devillers, J. *Neural Networks in QSAR and Drug Design*; Devillers, J., Ed.; Academic Press: New York, 1996.
- (36) Murata, N.; Yoshizawa, S.; Amari, S. Network Information Criterion – Determining the Number of Hidden Units for an Artificial Neural Network Model. *IEEE Trans. Neural Networks* **1994**, 5(6), 865–872.
- (37) Bursi, R.; Dao, T.; van Wilk, T.; de Gooyer, M.; Kellenbach, E.; Verwer, P. Comparative spectra analysis (CoSA): Spectra as three-dimensional molecular descriptors for the prediction of biological activities. *J. Chem. Inf. Comput. Sci.* **1999**, 39, 861–867.
- (38) Turner, D. B.; Willett, P.; Ferguson, A. M.; Heritage, T. Evaluation of novel infrared range vibration-based descriptor (EVA) for QSAR studies. 1. General application. *J. Comput.-Aided Design* **1997**, 11, 409–422.

CI025511E